


1
2
3
4 **Computational model of extracellular glutamate in the nucleus accumbens**
5
6
7 **predicts neuroadaptations by chronic cocaine**
8
9

10 Sandeep Pendyam^{1*}, Ashwin Mohan^{1*}, Peter W Kalivas², Satish S Nair¹
11
12
13

View metadata, citation and similar papers at core.ac.uk

brought to you by  CORE

provided by University of Missouri: MOspace

16 65201 Department of Neurosciences², Medical University of South Carolina, Charleston, SC
17

18 29425
19

20
21 * These authors contributed equally to the research.
22

23 **Abbreviated Title:** Modeling cocaine effect on glutamate
24

25 **Correspondence may be sent to:**
26

27
28 Peter Kalivas, Ph.D.
29 Department of Neurosciences
30 Medical University of South Carolina, Charleston, SC, 29425
31 Tel: 843-792-4400
32 Fax: 843-792-4423
33 Email: kalivasp@musc.edu
34
35
36
37
38

39 **Pages** 36
40

41 **Figures** 4
42

43 **Tables** 3
44

45 **Abstract** 237 words
46
47

48 **Introduction** 497 words
49

50 **Discussion** 1332 words
51
52

53 **Supplement** 3 figures, 2 tables, discussion
54
55

56 **Section Editor: Geoffrey Schoenbaum**
57
58
59
60
61
62
63
64
65

Acknowledgements: This research was supported in part by USPHS grants DA015369, DA03906 (PWK), and subcontract from DA015369 to University of Missouri (SSN).

LIST OF ABBREVIATIONS

mGluR2/3, metabotropic glutamate receptors;

xc-, Cystine-glutamate exchange;

XAG, Glutamate transporters;

PFC, Prefrontal cortex;

P_{syn} , P_{mGluR} , and P_{ex} , Glutamate concentrations at synapse, mGluR and extracellular space;

G_i , Glial sheath;

D_{syn} , D_{sh} and D_{ex} , Diffusion coefficient in the synapse, between the sheath and extracellular space;

TTX, Tetrodoxin;

AMPA, alpha-amino-3-hydroxy-5-methyl-4-isoxazolepropionic acid;

NMDA, N-methyl-D-aspartic acid;

GLT1, glial glutamate transporter protein

ABSTRACT

Chronic cocaine administration causes instability in extracellular glutamate in the nucleus accumbens that is thought to contribute to the vulnerability to relapse. A computational framework was developed to model glutamate in the extracellular space, including synaptic and nonsynaptic glutamate release, glutamate elimination by glutamate transporters and diffusion, and negative feedback on synaptic release via metabotropic glutamate receptors (mGluR2/3). This framework was used to optimize the geometry of the glial sheath surrounding excitatory synapses, and by inserting physiological values, accounted for known stable extracellular, extrasynaptic concentrations of glutamate measured by microdialysis and glutamatergic tone on mGluR2/3. By using experimental values for cocaine-induced reductions in cystine-glutamate exchange and mGluR2/3 signaling, the computational model successfully represented the experimentally observed increase in glutamate that is seen in rats during cocaine-seeking. This model provides a mathematical framework for describing how pharmacological or pathological conditions influence glutamate transmission measured by microdialysis.

-147 words-

Key words: Glutamate transporter, Glial geometries, Cystine-glutamate exchange, mGluR2/3, Non-synaptic release, Microdialysis

1
2
3
4 Repeated cocaine administration causes enduring changes in glutamate transmission in the
5
6 nucleus accumbens that may contribute to relapse vulnerability (Kalivas et al., 2005). These
7
8 changes include alterations in glutamate release (McFarland et al., 2003), postsynaptic glutamate
9
10 signaling (Conrad et al., 2008), dendritic spine morphology (Robinson and Kolb, 2004), and
11
12 group II metabotropic glutamate receptors (mGluR2/3; Xi et al., 2002). The diversity of
13
14 neuroadaptations has proven difficult to synthesize into a portrait of cocaine-induced pathology.
15
16 While obtaining experimental measurements of glutamate transmission is critical, an alternate
17
18 approach is to mathematically model an ‘archetypal’ synapse by extracting common features of
19
20 the synaptic environment from a large number of synapses (Clements et al., 1992; Kleinle et al.,
21
22 1996; Rusakov and Kullmann, 1998; Rusakov, 2001; Barbour, 2001; Diamond, 2005; Saftenku,
23
24 2005). These models have focused on synaptic glutamate release, diffusion out of the synapse
25
26 and elimination by glutamate transporters (XAG) in an effort to understand the accessibility of
27
28 synaptically released glutamate to the extracellular environment.
29
30
31
32
33
34
35
36
37

38 The mathematical models cited are based upon *in vitro* electrophysiological research and are
39
40 appropriate for assessing concentrations of glutamate in the synaptic cleft and the near adjacent
41
42 perisynaptic environment. However, *in vivo* extrasynaptic concentrations assessed by
43
44 microdialysis reveal that the majority of glutamate outside of the synaptic cleft is not of synaptic
45
46 origin (Miele et al., 1996; Timmerman and Westerink, 1997; Melendez et al., 2005). Also,
47
48 extracellular glutamate in tissue slices and cell culture experiments is partly of nonsynaptic
49
50 origin (Jabaudon et al., 1999; Haydon, 2001; LeMeur et al., 2007). While a number of sources of
51
52 nonsynaptic extracellular glutamate have been suggested (Danbolt, 2001; Haydon, 2001;
53
54 Cavelier et al., 2005), extracellular glutamate measured by microdialysis in the accumbens arises
55
56
57
58
59
60
61
62
63
64
65

1
2
3
4 primarily from cystine-glutamate exchange (xc-; Baker et al., 2002; Xi et al., 2002). Cystine-
5
6 glutamate exchange is the rate-limiting step in glutathione synthesis (McBean, 2002), and
7
8 glutamate derived from xc- stimulates perisynaptic mGluR2/3, and thereby inhibits synaptic
9
10 glutamate release (Xi et al., 2002; Moran et al., 2005).
11
12
13
14

15
16 These data indicate that mathematical modeling of glutamate transmission should include
17
18 nonsynaptic sources of glutamate. Moreover, rats withdrawn from chronic cocaine administration
19
20 show dysregulation of extracellular glutamate in the nucleus accumbens due, in part, to reduced
21
22 xc- and mGluR2/3 signaling (Baker et al., 2003; Madayag et al., 2007). Therefore, including
23
24 extrasynaptic glutamate is required to model relevant cocaine-induced neuroplasticity. Also,
25
26 while mathematical models considering only synaptically released glutamate predict that each
27
28 glutamate synapse functions in relative isolation from other synapses (Kleinle et al., 1996;
29
30 Barbour, 2001; Lehre and Rusakov, 2002; Sykova, 2004), microdialysis during cocaine-seeking
31
32 measures significant overflow of synaptic glutamate (McFarland et al., 2003, 2004).
33
34
35
36
37
38
39
40

41 In order to predict cocaine-induced adaptations in extracellular glutamate, we modeled synaptic
42
43 glutamate transmission, different glial geometries populated with XAG and xc-, and the
44
45 regulation of glutamate release by mGluR2/3. Combining physiological values from the literature
46
47 and empirically derived changes produced by chronic cocaine, the proposed mathematical
48
49 framework was able to accurately portray both basal and cocaine altered extracellular glutamate
50
51 levels as measured by microdialysis.
52
53

54 -497 words-
55
56
57
58
59
60
61
62
63
64
65

EXPERIMENTAL PROCEDURES

Model inputs and baseline diffusion, binding and transport parameters.

Baseline physiological parameters for glutamate transmission were employed, primarily as described in previous models of glutamate transmission (table 1). The principal mechanisms involved in transient glutamate dynamics in the perisynaptic region are glutamate diffusion out of the synapse after release, binding to transporters and uptake into glia (Danbolt, 2001), production of glutamate by the xc- located in glia (Pow, 2001; Sato et al., 2002), and activation of mGluR2/3 autoreceptors reducing synaptic release probability (Dietrich et al., 2002; Losonczy et al., 2003; Billups et al., 2005).

(table 1 approximately here)

Synaptic release and regulation by mGluR2/3 autoreceptors. *In vivo* estimates of basal firing frequency in prefrontal cortical (PFC) neurons projecting to the nucleus accumbens range from 1 to 3 Hz with the capacity for periods of burst firing up to 15 Hz (Chang et al, 1997; Peters et al., 2005; Sun and Rebec, 2006). Although the probability that an action potential will release a synaptic vesicle can range from <0.1 to 1 depending upon the experimental preparation (Allen and Stevens, 1994; Murthy and Sejnowski, 1997), the average synaptic release probability more typically ranges from 0.1 to 0.5, with estimates for cortex being at ~0.4 (Trommerhauser et al., 2003; Billups et al., 2005; Volynski et al., 2006). Release probability at glutamatergic synapses is reduced by up to 50% following stimulation of presynaptic mGluR2/3 autoreceptors (Dietrich et al., 2002; Losonczy et al., 2003; Billups et al., 2005), which are located outside of the synaptic cleft (Alagarsamy et al., 2001). Using *in vivo* microdialysis it has been shown that blocking mGluR2/3 elevates extracellular concentrations of glutamate (Xi et al., 2002) and

1
2
3
4 electrophysiological studies in tissue slices reveal that the glutamate providing this tone is
5
6 derived primarily from nonsynaptic sources (Bandrowski et al., 2003; Moran et al., 2005). Given
7
8 these studies indicating that partial tone exists on mGluR2/3 regulating glutamate release, the
9
10 basal levels of glutamate in the vicinity of perisynaptic mGluR2/3 were optimized in the present
11
12 model to produce ~50% occupancy, based upon the range of K_d and K_i values reported at this
13
14 receptor (0.1 to 0.3 μM glutamate; Schoepp and True, 1992). In the proposed model, presynaptic
15
16 tone on mGluR2/3 was computed as release probability. mGluR2/3 is a Gi-coupled metabotropic
17
18 receptor, and analysis of GTP γ S binding reveals that G protein signaling by stimulating
19
20 mGluR2/3 is increased as a logarithm of agonist dose (Xi et al., 2002; Bowers et al., 2004). Thus,
21
22 the relationship between release probability and mGluR2/3 occupation was modeled as the
23
24 logarithm of glutamate concentration, with a $K_d = 0.187 \mu\text{M}$ glutamate (Schoepp and True, 1992)
25
26 and maximum release probability with no mGluR2/3 stimulation set at 0.4 (see above). Each
27
28 action potential provoking glutamate release (a function of firing frequency and release
29
30 probability) resulted in an instantaneous vesicular release of a fixed number of molecules into the
31
32 cleft. This fixed number was selected iteratively from the range 4700-80,000 reported by Bruns
33
34 and Jahn (1995) and set at 10,000 (table 1).
35
36
37
38
39
40
41
42
43
44

45
46 *Diffusion.* In a complex medium, several factors can impose constraints on diffusion, including
47
48 geometry, binding, uptake, viscosity, temperature, or change in structure with time (Nicholson,
49
50 2001, Sykova, 2004, Diamond, 2005, Saftenku, 2005). Diffusion in the extracellular space is
51
52 typically characterized by volume fraction α (void space/total tissue volume) and tortuosity λ
53
54 (hindrance to diffusion imposed by local boundaries or local viscosity) (Nicholson, 2001).
55
56 Volume fraction α in brain tissue is estimated to be around 0.2 (Nicholson and Sykova, 1998).
57
58
59
60
61
62
63
64
65

1
2
3
4 Tortuosity λ varies due to constriction, wiggle and topological factors (Nicholson, 2001) and is
5
6 estimated to be $\sim 1.2-2.4$ based on diffusion measurements over a range of 100-300 μm
7
8 (Nicholson, 2001). To account for the complex factors cited, diffusion coefficient values have
9
10 been reported in the range from 0.05-0.41 $\mu\text{m}^2/\text{ms}$ (Saftenku, 2005), based on typical tortuosity
11
12 estimates. Further, different cellular elements including spines, small axonal boutons, protein,
13
14 glia, and microfilaments may result in additional tortuosity in the microenvironment of a synapse
15
16 (Saftenku, 2005). Experimental estimates of diffusion coefficients in the perisynaptic region have
17
18 not been reported for synapses with tightly packed glia. In the proposed model, with high density
19
20 glia close to the synapse, we iteratively determined the diffusion coefficients to satisfy steady
21
22 state and transient constraints on glutamate concentrations at three locations (P_{syn} , P_{mGluR} , and P_{ex}
23
24 in figure 1). This iterative process is described in more detail below.

25
26
27
28
29
30
31 *(Fig.1 approximately here)*

32
33
34 *Glutamate transporters (XAG)*. Glutamate transport into glia is the primary mechanism for
35
36 eliminating extracellular glutamate (Danbolt, 2001). XAG uptake rates depend on local
37
38 glutamate concentration and the kinetics of transporter binding (see eqn. 3 below). The
39
40 glutamatergic axon terminals from the PFC to the accumbens were assumed to be covered by a
41
42 glial sheath (Lehre et al., 1995). The density of XAG is non-uniform, and glial membranes that
43
44 face neuropil have a higher expression of transporters than membrane surfaces facing other glia
45
46 (Cholet et al., 2002). XAG are expressed with a high density in the hippocampus, with surface
47
48 density ranging from 2500-10,800 molecules/ μm^2 (Bergles and Jahr, 1997; Lehre and Danbolt,
49
50 1998). Based upon glutamate uptake assays (Colombo, 2005) and transporter binding studies
51
52 (Danbolt, 2001) it was estimated that surface density values for XAG in the nucleus accumbens
53
54 is 22-35% (550-3780 molecules/ μm^2) of the value in the hippocampus and cortex. Thus, for the
55
56
57
58
59
60
61
62
63
64
65

1
2
3
4 present model (where XAG is volume populated as described later), the equivalent surface
5
6 density of XAG was determined iteratively by varying it within the range of 550-3780
7
8 molecules/ μm^2 (table 1).
9

10
11
12
13
14 *Cystine-glutamate exchangers (xc-)*. Wyatt et al. (1996) estimated the maximum uptake rate for
15
16 cystine to be $450 \mu\text{mol l}^{-1}\text{hr}^{-1}$ based on cerebellar slices. The density of xc- in the cortex is higher
17
18 by a factor of 2.4 compared to the cerebellar molecular layer ($1 \text{ mmol l}^{-1}\text{hr}^{-1}$; Warr et al. 1999).
19
20 Based on microdialysis studies, Baker et al. (2003) reported basal extracellular glutamate
21
22 concentrations to be 1.1 and $5.6 \mu\text{M}$ in the prefrontal cortex and nucleus accumbens,
23
24 respectively. Iterations to satisfy model constraints resulted in the consideration of a range from
25
26 $5 - 50 \text{ mmol l}^{-1}\text{hr}^{-1}$ for the density of xc- in the nucleus accumbens and a final value of 41 mmol
27
28 $\text{l}^{-1}\text{hr}^{-1}$ under basal conditions (table 1).
29
30
31
32
33
34
35

36 **Model inputs and cocaine-induced neuroadaptations.**

37
38 The parameters adjusted in the model to estimate neuroadaptive changes produced by withdrawal
39
40 from chronic cocaine are outlined in table 2. Withdrawal from daily cocaine administration
41
42 elicits a 50% reduction in K_m for $[^{35}\text{S}]$ cystine uptake into accumbens tissue slices (Baker et al.,
43
44 2003), thereby decreasing the concentration of xc- by 50% (table 2). Previous studies using
45
46 $[^{35}\text{S}]\text{GTP}\gamma\text{S}$ binding in accumbens homogenates revealed that G protein coupling to mGluR2/3 is
47
48 reduced by approximately 70% after cocaine (Xi et al., 2002). Assuming a logarithmic
49
50 relationship between $[^{35}\text{S}]\text{GTP}\gamma\text{S}$ binding and vesicle release probability (see above), the
51
52 cocaine-induced reduction in mGluR2/3 function was modeled as a change in release probability
53
54 from 0.14 (control) to 0.34 (cocaine treated condition). Thus, a release event occurred every 2.9
55
56
57
58
59
60
61
62
63
64
65

1
2
3
4 action potentials in the cocaine case, instead of every 7.1 action potentials under basal
5
6 conditions. Finally, the firing frequency of pyramidal cells in the PFC during cocaine-seeking, a
7
8 portion of which project to the accumbens, increases from a range of 1-3 Hz to between 10-15
9
10 Hz (Sun and Rebec, 2006). Thus, to model activity at the glutamatergic synapse in the
11
12 accumbens between the basal and cocaine- or food-seeking condition, the firing frequency was
13
14 increased from 1-15 Hz.
15
16

17
18
19 *(table 2 approximately here)*
20

21 **Modeling the synapse and glial geometry.**

22
23 Upon release at the center of the synapse, glutamate molecules diffuse through the porous cleft
24
25 into the perisynaptic space (Barbour and Hausser, 1997), where XAG dense astrocytes reduce
26
27 glutamate spillover to near zero (Diamond and Jahr, 2000; Danbolt 2001). The configuration of
28
29 the glial sheath (G_i in figure 1) is akin to that previously reported (Rusakov, 2001), but distinct in
30
31 that in the present model we include xc-. Also, as an approximation of glial folds, the glial
32
33 membranes were modeled in the form of multiple impermeable sheaths (the dark line at the
34
35 center of each sheath in figure 1 represents an impermeable surface, i.e., flux=0 across this
36
37 surface) with porous space in between them. XAG was volume populated on both sides of each
38
39 glial sheath G_i (permeable to glutamate up to 25 nm thickness on each side of the impermeable
40
41 center surface of the 50 nm thick G_i). Glutamate concentration at mGluR2/3 receptors was
42
43 monitored in the model at the presynaptic location P_{mGluR} in figure 1 (compartment $i, j = 1, 2$,
44
45 starting at $\theta=20^\circ$).
46
47
48
49
50
51
52
53
54
55

56 The extracellular space is thus modeled as a porous medium with four glial sheaths whose
57
58 centerlines were 75 nm apart (close to the range of 38-64 nm reported in the extracellular space
59
60
61
62
63
64
65

of the rat neocortex *in vivo* by Thorne and Nicholson, 2006). Of this 75 nm, 50 nm is volume populated with XAG and/or xc-, as described above. This permits the glutamate molecules to move up to 75 nm between the impermeable surfaces of each sheath. Based upon studies indicating that the highest densities of XAG are closer to the synapse (Lehre and Danbolt, 1998; Danbolt, 2001; Cholet et al., 2002), G₁ had the highest density of XAG and the density decreased radially outwards to G₄. Cystine-glutamate exchangers were modeled as being located on the outer surface of the glial membranes of regions G₄ (table 1). Beyond the last glial sheath (G₄), the extracellular space contained only glutamate without XAG or xc-. The experimentally defined concentrations of extracellular glutamate reported by *in vivo* microdialysis (table 2) were modeled as being at point P_{ex} in figure 1, outside glial region G₄.

Mathematical details. In the configuration of figure 1, the two synaptic hemispheres were assumed rigid permitting no diffusion (i.e., flux = 0 along the periphery), with synaptic radius $r = 160$ nm from the center, and a separation of $\delta = 20$ nm (synaptic cleft) (Rusakov and Kullmann, 1998; Rusakov, 2001; Diamond, 2005). Around this synapse are 40 concentric 25 nm thick shell compartments ($i_1 - i_{40}$) resulting in the outer boundary of the perisynaptic region modeled being at a distance of 1 μ m from the edge of the synapse. Each of these shells was divided into 9 compartments (20° angle increments, $j_1 - j_9$) circumferentially, permitting XAG and xc- concentrations to be assigned individually to each compartment of any shell.

The synaptic cleft volume was discretized into $m = (1 \dots N_m)$ segments where dR_m was the outer radius ($R_m = m * dR_m$) of the cylindrical elements of thickness δ , each with a volume of $\pi(R_m^2 - R_{m-1}^2) * \delta$, with the contact surface between adjacent elements being $S_m = 2\pi R_m * \delta$. The

extracellular space were discretized into $i = (1...N_i)$ concentric spherical elements each of thickness σ , and each spherical element was divided into $j = (1...N_j)$ annular sections where N_j was determined by θ . In the model for the cleft, $m=4$, and $dR_m = 40$ nm, and for the spherical shells, $\sigma=25$ nm and $\theta = \pi/9$ rad.

The specific mathematical equations used are described next. These standard conservation and flux equations (see Rusakov, 2001 for a comprehensive description including derivations) were used to analyze the effect of the proposed glial geometry. A mass balance for extracellular glutamate in each $(i,j)^{th}$ compartment (with XAG and/or xc-, as appropriate) yields eqn.1 (Rusakov, 2001),

$$Glu(i, j, t) = Glu(i, j, t - dt) + (J_R \Sigma(i, j, t) S_R + J_T \Sigma(i, j, t) S_T) \frac{dt}{V(i, j)} + (v_+ - v_-) dt \quad (1)$$

where dt was the time step, $S_R(i, j) = 2\pi R_i^2 (\cos \theta_j - \cos \theta_{j-1})$ was the surface area between adjacent volume elements in the radial direction, and $S_T(i, j) = 2\pi R_i \sin \theta_j * (\sigma)$ was the surface area shared by adjacent volume elements in the tangential direction, with $R_i = r + \sigma * i$. The radial and tangential fluxes into the compartment were denoted by J_R and J_T , respectively. Each compartment had a volume of $V(i, j) = 0.5(S_R(i, j) + S_R(i-1, j)) * (\sigma)$. The term v_+ accounted for the production of glutamate by xc- and unbinding of glutamate from the transporters ($v_+ = cg(i, j) + k_l * [Glu-XAG]$, where $cg(i, j)$ is the constant production rate of glutamate by xc- for compartment (i, j) , while the term ($v_- = k_l * [Glu] * [XAG]$) accounted for the reduction in glutamate due to transporter binding. For compartments that are not populated with XAG or xc-, the corresponding terms in eqn. 1 are omitted. Also, eqn.1 is appropriately modified for the compartments in the synaptic cleft, to exclude XAG, xc-, and the tangential flux, and include synaptic release.

The glutamate flux J_{AB} between any two adjacent volume compartments A and B was computed by eqn. 2,

$$J_{AB}(t) = -D\nabla(Glu) = -\frac{D}{ds}(Glu_A(t-dt) - Glu_B(t-dt)) \quad (2)$$

where ds was the spatial distance between compartment centroids and D the diffusion coefficient. For each compartment, this flux was calculated considering two others connected to it radially, and two connected in the tangential direction. Within any glial compartment, binding of glutamate with transporters is governed by eqn. 3, (Rusakov and Kullmann, 1998),



where $[Glu]$, $[XAG]$, and $[Glu-XAG]$ represent the compartmental concentrations of glutamate, transporter, and the bound complex, respectively, and $k_2*[Glu_{in}]$ represents uptake rate of glutamate by XAG.

The discrete form of the differential equation for this kinetic equation is given by eqn. set 4 (Rusakov, 2001):

$$\begin{aligned} [Glu]_t &= [Glu]_{t-dt} + (-k_1[Glu]_{t-dt}[XAG]_{t-dt} + k_{-1}[Glu - XAG]_{t-dt})dt \\ [Glu - XAG]_t &= [Glu - XAG]_{t-dt} + \{-(k_{-1} + k_2)[Glu - XAG]_{t-dt} + k_1[Glu]_{t-dt}[XAG]_{t-dt}\}dt \\ [Glu - XAG]_t + [XAG]_t &= [Glu - XAG]_{t-dt} + [XAG]_{t-dt} = [XAG_{total}] \\ [Glu_{in}]_t &= [Glu_{in}]_{t-dt} + k_2 * [Glu - XAG]_{t-dt} * dt \end{aligned} \quad (4)$$

The kinetics for XAG were taken from Rusakov (2001) and Lehre and Rusakov (2002) who based it on experiments reported in the literature (Wadiche et al., 1995; Bergles and Jahr, 1998), $k_1 = 10^4 \text{ M}^{-1}\text{ms}^{-1}$, $k_{-1} = 0.2 \text{ ms}^{-1}$, and $k_2 = 0.1 \text{ ms}^{-1}$. For the outermost shell, e.g., $i = 40$, the

1
2
3
4 boundary condition of flux = 0 was imposed at the outer edge of all compartments, to simulate
5
6 identical neighboring synapses. That is, no flux enters or leaves the outer boundary of this shell.
7
8
9

10
11 *Iterative evaluation.* The computational model was developed using C⁺⁺ software (Microsoft
12 Visual Studio, 2005), and an integration time step of 0.5 μ s was used. The concentration of
13
14 glutamate was considered uniform in each compartment and this concentration was updated
15
16 (eqns. 1-4) at each integration interval based on diffusion, uptake by XAG, and production rates
17
18 for glutamate, as appropriate. Conservation of molecules was confirmed at each time step by
19
20 computing the numbers of free, bound and transported glutamate molecules. To check for
21
22 numerical accuracy, we decreased the integration time step by a factor of 10 and found no
23
24 significant change in concentration estimates. Similarly, insignificant changes in the same
25
26 estimates were found with variation of spatial resolution of compartments by 50%.
27
28
29
30
31
32
33
34
35

36 To implement a volume fraction of $\alpha = 0.2$ (Nicholson and Sykova, 1998) in the model shown in
37
38 figure 1 (which was also iteratively derived; details not shown), we approximated shells $i=20-40$
39
40 to be representing cellular obstacles (i.e., space that glutamate cannot flow into), with an
41
42 effective extracellular space from $i=1-20$ for glutamate overflow. This implies that P_{ex} is now
43
44 measured in shell 20. The model showed that in the space outside the glial sheaths (i.e., outside
45
46 shell 12) the steady state concentration of glutamate was uniform for any number of total outside
47
48 shells, and differed by less than 0.01 μ M for all cases considered. This observation justifies
49
50 selection of P_{ex} anywhere in the space outside G_4 for measurement purposes.
51
52
53
54
55
56
57
58
59
60
61
62
63
64
65

1
2
3
4 As cited earlier, diffusion coefficients close to the synapse have not been reported for synapses
5
6 with tight glial coverage. With the glial geometry in figure 1, we considered three diffusion
7
8 coefficients, one in the synapse (D_{syn} near P_{syn}), one in the sheath region (D_{sh} in the region that
9
10 has P_{mGluR}) and one outside the glial sheath region (D_{ex} in the region that has P_{ex}). We noticed
11
12 that the flow dynamics was governed solely by D_{sh} , with insignificant effects due to variations in
13
14 D_{syn} and D_{ex} within the range of 0.05 to 0.41 $\mu\text{m}^2/\text{ms}$ (data not shown). Accordingly, we used a
15
16 uniform value of D (from the same range cited above) for all the regions in the model, without
17
18 loss of accuracy. It should be noted that the glial sheaths added geometric tortuosity in the model.
19
20
21
22
23
24
25

26 The model was optimized by changing the following parameters within the ranges outlined in
27
28 table 1: number of molecules/release, xc- concentration, diffusion coefficient and XAG
29
30 concentration. The iterative process began with values in the lower end of the ranges for these
31
32 parameters, while monitoring the concentrations of glutamate at P_{syn} , P_{mGluR} , and P_{ex} (figure 1),
33
34 for the basal control case (2 Hz). When the densities of XAG were iteratively changed in glial
35
36 sheaths G_i , their relative proportions were maintained, i.e., density (G_1) > density (G_2) and so on.
37
38 Through this iterative process, numerous solutions were found that satisfied empirically
39
40 determined concentrations at P_{syn} , P_{mGluR} , and P_{ex} for the control case at 2 Hz (table 2).
41
42
43
44
45
46
47

48 After satisfying the requirements for the basal control case, we simulated the basal cocaine and
49
50 drug-seeking situation by modeling known cocaine-induced changes to xc- and mGluR2/3
51
52 signaling (modeled as release probability, see above). Through further iterative changes we
53
54 identified multiple parameter sets that satisfied some of the constraints in table 2, and the model
55
56 values listed in table 1 constitute values that satisfied all the constraints simultaneously.
57
58
59
60
61
62
63
64
65

RESULTS

Geometry of the glial sheath. Multiple 3-D spherical configurations were studied for glia surrounding the synapse by varying glial coverage, thickness and openings (similar to those in Rusakov, 2001; Barbour, 2001; data not shown). Table 1 shows the range of diffusion coefficients, number of molecules per release, as well as XAG and xc- concentrations in the various glial sheaths. These were varied iteratively to determine the configuration that brought glutamate concentration at P_{ex} (extracellular compartment sampled by microdialysis) into the range outlined in table 2 at both low and high firing frequencies. At the same time, concentrations at P_{syn} and P_{mGluR} were constrained to be <200 nM. This process involved simultaneous variations of the parameters (see Methods). Following this iterative process, the configuration in figure 1 proved most robust at sustaining glutamate concentrations within the acceptable ranges. Of note, the basal control concentration at P_{ex} did not exceed the range measured by microdialysis at firing frequencies of 15 Hz (table 3, figure 2A). Also, by providing resistance to the flow of glutamate, this configuration established the necessary gradient to support levels of extracellular glutamate at P_{syn} approaching those estimated from *in vitro* slice physiology (Herman and Jahr, 2007) and at P_{mGluR} that are consistent with *in vivo* tone being present on mGluR2/3 (Xi et al., 2002). Thus, at both low and high frequency stimulation, P_{mGluR} remained between 0.1 and 0.3 μ M, which approximates the K_d for glutamate binding to mGluR2/3 (0.19 μ M; Schoepp and True, 1992).

(Fig 2 approximately here) + (table 3 approximately here)

Figure 2B shows how the increase in P_{mGluR} associated with increased firing frequency negatively regulated release probability, i.e., as P_{mGluR} increased with increasing synaptic release, the release probability decreased from 0.14 to 0.12. Thus, as firing frequency ranged from 1 to 15

1
2
3
4 Hz, the peak concentration at P_{syn} reached as high as 10 mM, which, when averaged over 100 μs
5
6 around this peak, resulted in a maximum value of 0.5 mM (figure 2C). As well, transient
7
8 glutamate concentrations in the synapse (at P_{syn}) were biphasic and within ranges reported by
9
10 Clements (1996) and Bergles et al. (1999). The resting concentration at P_{syn} between release
11
12 events ranged from 0.16 to 0.19 μM (table 3). These levels are somewhat higher than recent
13
14 published estimates which range from 25 to 100 nM using tonic activity at NMDA receptors in
15
16 tissue culture (Herman and Jahr, 2007; Le Meur et al., 2007), and could reflect a lack of neuronal
17
18 glutamate uptake in the present model.
19
20
21
22
23
24
25

26 **Effect of withdrawal from chronic cocaine.**

27
28 Table 2 illustrates the alterations made in parameters by incorporating experimentally determined
29
30 values for reduced xc- and mGluR2/3 desensitization after chronic cocaine (Xi et al., 2002;
31
32 Baker et al., 2003). In addition, concentrations at P_{ex} approximated the basal values determined
33
34 by microdialysis in the accumbens after withdrawal from chronic cocaine, as well as peak values
35
36 elicited after inducing cocaine-seeking. The transition from basal to cocaine-seeking behavior is
37
38 associated with an increase in firing frequency of accumbens neurons, driven in part by inputs
39
40 from the prefrontal cortex, and the firing frequency can range from 1 to 15 Hz (Sun and Rebec,
41
42 2006), while the *in vivo* basal firing of prefrontal pyramidal cells is reduced after withdrawal
43
44 from self-administered cocaine (Trantham et al., 2002; however, see Dong et al., 2005, showing
45
46 increased excitability of dissociated prefrontal pyramidal cells after chronic cocaine). Therefore,
47
48 to model this behavioral transition, a firing frequency range of 1 (basal) to 15 Hz (cocaine-
49
50 seeking) was employed. The model constraints for the basal extracellular concentration measured
51
52 by dialysis in P_{ex} after cocaine was in the range of 2.55-3.23 μM , and the basal concentration for
53
54
55
56
57
58
59
60
61
62
63
64
65

1
2
3
4 control animals was in the range of 4.6-6.6 μM (Baker et al., 2003; Szumlinski et al., 2006).
5
6 When cocaine-seeking was introduced into the model (i.e., 15 Hz firing frequency) extracellular
7
8 concentration was expected to be in the range of 11.9-14.7 μM (McFarland et al., 2003, 2004;
9
10 Szumlinski et al., 2006). In contrast, in control animals engaging in the seeking of biological
11
12 rewards (e.g., food), the level of extracellular glutamate at P_{ex} is not expected to differ
13
14 significantly from basal (i.e., remain in the range of 4.6-6.6 μM ; McFarland et al., 2003).
15
16

17
18
19 *(figures 3 and 4 approximately here)*
20

21 Figures 3 and 4 illustrate the outcome for concentrations at P_{syn} and P_{ex} after introducing the
22
23 cocaine-altered parameters for xc- and mGluR2/3 (modeled as release probability, see Methods)
24
25 and stimulating synaptic transmission at 1 to 15 Hz. Over a firing frequency of 1 to 15 Hz, the
26
27 change in concentration at P_{mGluR} was similar to that at P_{syn} (table 3). While the model accurately
28
29 predicted the reduction in basal value at P_{ex} into the expected range, it did not predict the
30
31 expected increase in the concentration at P_{ex} for the 15 Hz case (see 0% reduction in XAG in
32
33 figure 3). Although values after chronic cocaine for both xc- and mGluR2/3 regulation of release
34
35 probability have been empirically determined, no experimental values for XAG after withdrawal
36
37 from cocaine have been published. Thus, the model was employed to iteratively explore the
38
39 effects of changing XAG, and it was found that if XAG was reduced in the range of 40-50%, the
40
41 concentration at P_{ex} rose with increasing firing frequency to within the expected range of 11.9-
42
43 14.7 μM (figure 3). Figure 4 shows modeled data including a 40% reduction in XAG along with
44
45 the cocaine-induced reductions in xc- and mGluR2/3 signaling. Note that release probability did
46
47 not change appreciably even though P_{mGluR} increased as a function of increased firing frequency
48
49 due to the fact that mGluR2/3 signaling is reduced by 70% after chronic cocaine (Xi et al., 2002).
50
51
52
53
54
55
56
57
58
59
60
61
62
63
64
65

DISCUSSION

A computational modeling framework for studying glutamate homeostasis in prefrontal glutamatergic synapses onto nucleus accumbens spiny cells is reported that predicted extracellular glutamate concentrations as measured by *in vivo* microdialysis. The parameters used include those previously employed in computational models of excitatory neurotransmission, such as synaptic release, diffusion from the synaptic cleft and glutamate uptake, as well as parameters not typically modeled, including xc- and negative feedback on synaptic release by perisynaptic mGluR2/3. These latter parameters were included to model changes in extracellular glutamate concentrations produced by chronic cocaine administration that are hypothesized to result at least in part from cocaine-induced reductions in xc- and mGluR2/3 signaling (Xi et al., 2002; Baker et al., 2003; Moran et al., 2005). The computational model successfully predicted extracellular concentrations at different firing frequencies in control accumbens. Although incorporating cocaine-induced reductions in xc- and mGluR2/3 signaling predicted the reduction at P_{ex} at low firing frequencies, it was necessary to incorporate a reduction in XAG to predict the large increase at P_{ex} that occurs at the higher firing frequencies achieved during cocaine-seeking. Importantly, recent reports indicate that XAG is reduced in the accumbens after withdrawal from self-administered cocaine, including lower levels of the primary glial transporter, GLT-1, and a decrease in $^3[H]$ -glutamate uptake (Knackstedt et al., 2007).

Effect of chronic cocaine on glutamatergic transmission.

Withdrawal from repeated cocaine administration results in two changes in extracellular glutamate measured by microdialysis: 1) reduced basal concentrations, and 2) increased levels of glutamate after an acute injection of cocaine that induces cocaine-seeking or sensitized motor

1
2
3
4 activity (Pierce et al., 1996; Reid and Berger, 1996; Hotsenpiller et al., 2001; Baker et al., 2003;
5
6 McFarland et al., 2003; Madayag et al., 2007). Under basal conditions, glutamate measured by
7
8 microdialysis is almost entirely of nonsynaptic origin (Miele et al., 1996; Timmerman and
9
10 Westerink, 1997; Melendez et al., 2005), while the increase following a cocaine injection in
11
12 chronic cocaine treated animals is of synaptic origin (i.e., blocked by tetrodotoxin or inhibiting
13
14 prefrontal glutamatergic inputs to the accumbens; Pierce et al., 1996; McFarland et al., 2003).
15
16 Importantly, an increase in extracellular glutamate (either synaptic or nonsynaptic) does not
17
18 accompany an acute injection of cocaine or operant responding in animals trained to seek
19
20 biological rewards such as food (Pierce et al., 1996; Hotsenpiller et al., 2001; McFarland et al.,
21
22 2003). Thus, in the accumbens of animals chronically pretreated with cocaine, synaptic
23
24 glutamate transmission appears to escape from the immediate synaptic environment and is
25
26 measured in significant amounts outside of the synaptic region. The overflow of synaptic
27
28 glutamate in animals withdrawn from cocaine is in contrast to the lack of diffusion by significant
29
30 amounts of synaptic glutamate to adjacent synapses predicted under physiological conditions by
31
32 previous mathematical models (Barbour, 2001; Lehre and Rusakov, 2002; Sykova, 2004) or
33
34 empirically derived using *in vivo* microdialysis (Miele et al., 1996; Timmerman and Westerink,
35
36 1997; Melendez et al., 2005). Thus, it is possible that the cocaine-induced glutamate overflow
37
38 may be a critical event in addiction. However, stress induces overflow of glutamate in the
39
40 striatum or prefrontal cortex that is inhibited by TTX (Moghaddam, 2002), indicating that at least
41
42 some biological stimuli can also induce release of synaptic glutamate measurable by dialysis.
43
44
45
46
47
48
49
50
51
52
53
54
55
56
57
58
59
60
61
62
63
64
65

The concentrations of glutamate predicted by the model at P_{mGluR} and at P_{syn} are presumably capable of stimulating perisynaptic and synaptic glutamate receptors in adjacent synapses, since

1
2
3
4 at 15 Hz firing frequency (e.g., during drug-seeking), the model predicted that the concentration
5
6 of glutamate at P_{syn} and at P_{mGluR} are 1.1 and 1.2 μM , respectively, and the estimated K_d values
7
8 for mGluR2 and NMDA receptors are in the range of 200 nM and 2 μM , respectively (Patneau
9
10 and Mayer, 1990; Schoepp and True, 1992). Moreover, this concentration of glutamate would be
11
12 expected to partially desensitize NMDA receptors (Cavelier et al., 2005), and could contribute to
13
14 the increase in AMPA/NMDA current ratio (Kourrich et al., 2007) and AMPA receptor
15
16 membrane insertion seen after chronic cocaine (Conrad et al., 2005).
17
18
19
20
21
22

23 **Limitations of the proposed mathematical model.**

24
25 Two general limitations exist in the proposed model. The first limitation is the simplicity of the
26
27 model relative to the known physiology and cocaine-induced changes in glutamate transmission.
28
29 Notably, only occupancy of mGluR2/3 is considered, but occupancy of mGluR1 or mGluR5 can
30
31 be expected to change glutamate release and synaptic scaling (Malenka and Bear, 2004; Kreitzer
32
33 and Malenka, 2005), and mGluR1/5 content and/or function is altered by chronic cocaine
34
35 administration (Swanson et al., 2001; Szumlinski et al., 2006). In addition to xc-, there are other
36
37 sources of nonsynaptic glutamate release that may tonically stimulate glutamate receptors, such
38
39 as calcium-dependent release from astroglia and release from junction hemi-channels (Danbolt,
40
41 2001; Cavelier et al., 2005). Finally, while the glial geometry used in the framework is a
42
43 reflection of endogenous tortuosity, it oversimplifies the more varied *in vivo* structural geometry.
44
45 Thus, future models need to consider additional dynamic cellular processes that accompany
46
47 alterations in firing frequency, as well as more complicated morphological geometries.
48
49
50
51
52
53
54
55
56
57
58
59
60
61
62
63
64
65

1
2
3
4 A second important consideration is that in contrast to the standard mathematical models using
5
6 postsynaptic currents to empirically validate synaptic concentrations of extracellular glutamate,
7
8 the present model employed *in vivo* microdialysis measures. Although the strengths of
9
10 microdialysis are that estimates are made *in vivo* and nonsynaptic release is readily determined,
11
12 microdialysis induces damage artifacts that are distinct from the damage artifacts produced by
13
14 dissecting tissue for *in vitro* measurements. Two distinctions between estimates of extracellular
15
16 glutamate made *in vitro* versus with *in vivo* microdialysis are particularly relevant. The first is
17
18 that previous microdialysis estimates of extraction fraction (i.e. the slope of the line in the no net
19
20 flux experiment; Bungay et al., 2003), which is used to determine the elimination rate of
21
22 glutamate in brain tissue by passing different concentrations of glutamate through the probe,
23
24 found no apparent change in uptake (Baker et al., 2003). In contrast, both [³H]-glutamate uptake
25
26 and membrane protein content of GLT-1 are reduced ~40% in the accumbens (Knackstedt et al.,
27
28 2007). Recent modeling of microdialysis concludes that the extraction fraction may not be a
29
30 reliable estimate of transmitter uptake (Bungay et al., 2003; Chen, 2006). The reasons for this
31
32 are two-fold. 1) The presence of a tissue trauma layer changes the tissue resistance and volume in
33
34 the vicinity of the dialysis probe. While this markedly affects the estimates of extraction
35
36 fraction, it does not impact the no net flux estimate of basal transmitter concentration. 2) The
37
38 distribution of XAG within the present model is based upon data indicating that uptake sites are
39
40 concentrated in the vicinity of the synaptic cleft (Lehre and Danbolt, 1998; Danbolt, 2001), while
41
42 nonsynaptic glutamate release via xc⁻ was inversely distributed with the highest concentration of
43
44 xc⁻ being found away from the synapse (Sato et al., 2002). This distribution of XAG and xc⁻ can
45
46 contribute to both the lack of TTX sensitivity in basal glutamate levels and the relatively poor
47
48 capacity to detect uptake-dependent changes in the extraction fraction (Bungay et al., 2003).
49
50
51
52
53
54
55
56
57
58
59
60
61
62
63
64
65

1
2
3
4
5
6
7 The second concern raised by modeling glutamate transmission based upon microdialysis
8
9 measurements is revealed by estimates of extracellular glutamate using NMDA currents in tissue
10
11 slices being 1-3 orders of magnitude less than dialysis measurements (Cavelier et al., 2005;
12
13 Herman and Jahr, 2007). However, this fact is largely incorporated into the proposed model that
14
15 contains a steep gradient of glutamate concentrations between the synapse ($P_{mGluR} < 0.2 \mu M$ where
16
17 the electrophysiological measures are obtained) and the site where the dialysis measurements
18
19 occur ($P_{ex} = 5.04 \mu M$).
20
21
22
23
24
25

26 **Conclusions.**

27
28 A computational framework of glutamate transmission is presented that incorporates both
29
30 synaptic and nonsynaptic glutamate release and homeostatic regulation of synaptic release via
31
32 stimulation of mGluR2/3 autoreceptors. This model accurately predicted the basal levels of
33
34 extracellular glutamate measured by microdialysis, as well as the levels of glutamate in the
35
36 vicinity of mGluR2/3 that provides inhibitory tone on synaptic release. Thus, this model provides
37
38 a general mathematical framework for describing how pharmacological or pathological
39
40 conditions influence glutamate transmission, and for predicting molecular targets that may be
41
42 important to experimentally evaluate.
43
44
45
46
47

48 -1332 words-
49
50
51
52
53
54
55
56
57
58
59
60
61
62
63
64
65

REFERENCES

- 1
2
3
4
5
6
7 Alagarsamy S, Sorensen SD, Conn PJ (2001) Coordinate regulation of metabotropic glutamate
8 receptors. *Cur Op Neurobiol* 11:357–362.
9
10
11 Allen C, Stevens CF (1994) An evaluation of causes for unreliability of synaptic transmission.
12 *Proc Natl Acad Sci USA* 91: 10380-10383.
13
14
15 Baker DA, Xi ZX, Shen H, Swanson CJ, Kalivas PW (2002) The origin and neuronal function of
16 in vivo nonsynaptic glutamate. *J Neurosci* 22: 9134-9141.
17
18
19 Baker DA, McFarland K, Lake RW, Shen H, Tang XC, Toda S, Kalivas PW (2003)
20 Neuroadaptations in cystine-glutamate exchange underlie cocaine relapse. *Nat Neurosci*
21 6:743-749.
22
23
24 Bandrowski AE, Huguenard JR, Prince DA (2003) Baseline glutamate levels affect group I and
25 II mGluRs in layer V pyramidal neurons of rat sensorimotor cortex. *J Neurophysiol* 89:1308-
26 1316.
27
28
29 Barbour B (2001) An evaluation of synapse independence. *J Neurosci* 21: 7969-7984.
30
31
32 Barbour B, Hausser M (1997) Intersynaptic diffusion of neurotransmitter. *Tr Neurosci* 20:377-
33 384.
34
35
36 Bergles DE, Jahr CE (1997) Synaptic activation of glutamate transporters in hippocampal
37 astrocytes. *Neuron* 19:1297–1308.
38
39
40 Bergles DE, Jahr CE (1998) Glial contribution to glutamate uptake at schaffer collateral-
41 commissural synapses in hippocampus. *J Neurosci* 18:7709-7716.
42
43
44 Bergles DE, Diamond JS, Jahr CE (1999) Clearance of glutamate inside the synapse and beyond.
45 *Curr Op Neurobiol* 9:293–298.
46
47
48
49
50
51
52
53
54
55
56
57
58
59
60
61
62
63
64
65

- 1
2
3
4 Bowers MS, McFarland K, Lake RW, Peterson YK, Lapish CC, Gregory ML, Lanier SM,
5
6 Kalivas PW (2004) Activator of G-protein signaling 3: a gatekeeper of cocaine
7
8 sensitization and drug-seeking. *Neuron* 42: 269-281.
9
10
11 Billups B, Graham BP, Wong AY, Forsythe ID (2005) Unmasking group III metabotropic
12
13 glutamate autoreceptor function at excitatory synapses in the rat CNS. *J Physiol (Lond)*
14
15 565:885-896.
16
17
18
19 Bruns D, Jahn R (1995) Real-time measurement of transmitter release from single synaptic
20
21 vesicles. *Nature* 377: 62-65.
22
23
24 Bungay PM, Newton-Vinson P, Isele W, Garris PA, Justice Jr. JB (2003). Microdialysis of
25
26 dopamine interpreted with quantitative model incorporating probe implantation trauma. *J*
27
28 *Neurochem* 86: 932–946.
29
30
31 Cavelier P, Hamann M, Rossi D, Mobbs P, Attwell D (2005) Tonic excitation and inhibition of
32
33 neurons: ambient transmitter sources and computational consequences. *Prog Biophys Mol*
34
35 *Biol* 87: 3-16.
36
37
38 Chang JY, Zhang L, Janak PH, Woodward DJ (1997) Neuronal responses in prefrontal cortex
39
40 and nucleus accumbens during heroin self-administration in freely moving rats. *Brain Res*
41
42 754: 12–20.
43
44
45 Chen KC (2006) Effects of tissue trauma on the characteristics of microdialysis zero-net-flux
46
47 method sampling neurotransmitters. *J Theor Biol* 238: 863–881.
48
49
50 Cholet N, Pellerin L, Magistretti PJ, Hamel E (2002) Similar perisynaptic glial localization for
51
52 Na⁺, K⁺-ATPase alpha 2 subunit and the glutamate transporters GLAST and GLT-1 in the
53
54 somatosensory cortex. *Cereb Cortex* 12:515-525.
55
56
57
58
59
60
61
62
63
64
65

- 1
2
3
4 Clements JD, Robin A, Lester J, Tong G, Jahr CE, Westbrook GL (1992) The time course of
5
6 glutamate in the synaptic cleft. *Science* 258:1498-1501.
7
8
9 Clements JD (1996) Transmitter time course in synaptic cleft: its role in central synaptic
10
11 function. *Tr Neurosci* 19: 163-171.
12
13
14 Colombo JA (2005) Glutamate uptake by rat brain astroglia incubated in human cerebrospinal
15
16 fluid. *Med Sci Monitor* 11:BR13-7.
17
18
19 Conrad KL, Tseng KY, Uejima JL, Reimers JM, Hen LJ, Shaham Y, Marinelli M, Wolf ML
20
21 (2008) Formation of accumbens GluR2-lacking AMPA receptors mediates incubation of
22
23 cocaine seeking. *Nature*, in press.
24
25
26 Danbolt NC (2001) Glutamate uptake. *Prog Neurobiol* 65:1-105.
27
28
29 Diamond JS (2005) Deriving the glutamate clearance time course from transporter currents in
30
31 CA1 hippocampal astrocytes: transmitter uptake gets faster during development. *J Neurosci*
32
33 25:2906-2016.
34
35
36 Diamond JS, Jahr CE (2000) Synaptically released glutamate does not overwhelm transporters
37
38 on hippocampal astrocytes during high-frequency stimulation. *J Neurophysiol* 83: 2835-
39
40 2843.
41
42
43 Dietrich D, Kral T, Clusmann H, Friedl M, Schramm J (2002) Presynaptic group II metabotropic
44
45 glutamate receptors reduce stimulated and spontaneous transmitter release in human dentate
46
47 gyrus. *Neuropharmacol* 42:297-305.
48
49
50 Dong Y, Nasif FJ, Tsui JJ, Ju WY, Cooper DC, Hu XT, Malenka RC, White FJ (2005) Cocaine-
51
52 induced plasticity of intrinsic membrane properties in prefrontal cortex pyramidal neurons:
53
54 adaptations in potassium currents. *J Neurosci* 25:936-940.
55
56
57 Haydon P (2001) Glia: listening and talking to the synapse. *Nat Neurosci* 2:185-191.
58
59
60
61
62
63
64
65

- 1
2
3
4 Herman MA, Jahr CE (2007) Extracellular glutamate concentration in hippocampal slice. *J*
5
6 *Neurosci* 27: 9736-9741.
7
8
9 Hotsenpiller G, Giorgetti M, Wolf ME (2001) Alterations in behaviour and glutamate
10
11 transmission following presentation of stimuli previously associated with cocaine exposure.
12
13 *Eur J Neurosci* 14:1843-1855.
14
15
16 Jabaudon D, Shimamoto K, Yasuda-Kamatani Y, Scanziani M, Gahwiler BH, Gerber U (1999)
17
18 Inhibition of uptake unmasks rapid extracellular turnover of glutamate of nonvesicular origin.
19
20 *Proc Natl Acad Sci USA* 96:8733-8738.
21
22
23 Kalivas PW, Volkow N, Seamans J (2005) Unmanageable motivation in addiction: pathology in
24
25 prefrontal-accumbens glutamate transmission. *Neuron* 45:647-650.
26
27
28 Kleinle J, Vogt K, Luscher H -R., Muller R, Senn W, Wyler K, Streit J (1996) Transmitter
29
30 concentrations profiles in the synaptic cleft: an analytical model of release and diffusion.
31
32 *Biophys J* 71:2413-2426.
33
34
35 Knackstedt LA, Melendez R, Kalivas PW (2007) Cocaine self-administration alters the
36
37 expression of proteins associated with glutamatergic transmission and homeostasis at cortico-
38
39 accumbens synapses. Society for Neuroscience Annual Meeting, San Diego, CA: Abstract
40
41 815.8.
42
43
44 Kourrich S, Rothwell PE, Klug JR, Thomas MJ (2007) Cocaine experience controls bidirectional
45
46 synaptic plasticity in the nucleus accumbens. *J Neurosci* 27:7921-7928.
47
48
49 Kreitzer AC, Malenka RC (2005) Dopamine modulation of state-dependent endocannabinoid
50
51 release and long-term depression in the striatum. *J Neurosci* 25: 10537-10545.
52
53
54 Lehre KP, Levy LM, Ottersen OP, Storm-Mathisen J, Danbolt NC (1995) Differential expression
55
56 of two glial glutamate transporters in the rat brain: quantitative and immunocytochemical
57
58
59
60
61
62
63
64
65

1
2
3
4 observations. *J Neurosci* 15:1835-1853.
5

6
7 Lehre KP, Danbolt NC (1998) The number of glutamate transporter subtype molecules at
8
9 glutamatergic synapses: chemical and stereological quantification in young adult rat brain. *J*
10
11 *Neurosci* 18:8751-8757.
12

13
14 Lehre KP, Rusakov D (2002) Asymmetry of glia near synapse favors presynaptic glutamate
15
16 escape. *Biophys J* 83(1):125-134.
17

18
19 Le Meur K, Galante M, Anulo MC, Audinat E (2007) Tonic activation of NMDA receptors by
20
21 ambient glutamate of non-synaptic origin in the rat hippocampus. *J Physiol* 580.2: 373-383.
22

23
24 Losonczy A, Somogyi P, Nusser Z (2003) Reduction of excitatory postsynaptic responses by
25
26 persistently active metabotropic glutamate receptors in the hippocampus. *J Neurophysiol*
27
28 89:1910–1919.
29

30
31 Madayag A, Lobner D, Kau KS, Mantsch JR, Abdulhameed O, Hearing M, Grier MD, Baker DA
32
33 (2007) Repeated N-acetylcysteine administration alters plasticity-dependent effects of
34
35 cocaine. *J Neurosci* 27: 13968-13976.
36
37

38
39 Malenka RC, Bear MF (2004) LTP and LTD: an embarrassment of riches. *Neuron* 44: 5-21.
40

41
42 McBean GJ (2002) Cerebral cystine uptake: a tale of two transporters. *Tr Pharmacol Sci* 23:299-
43
44 302.
45

46
47 McFarland K, Lapish CC, Kalivas PW (2003) Prefrontal glutamate release into the core of the
48
49 nucleus accumbens mediates cocaine-induced reinstatement of drug-seeking behavior. *J*
50
51 *Neurosci* 23:3531-3537.
52

53
54 McFarland K, Davidge SB, Lapish CC, Kalivas PW (2004) Limbic and motor circuitry
55
56 underlying footshock-induced reinstatement of cocaine-seeking behavior. *J Neurosci*
57
58 24:1551-1560.
59
60
61
62
63
64
65

- 1
2
3
4 Melendez RI, Vuthiganon J, Kalivas PW (2005) Regulation of extracellular glutamate in the
5
6 prefrontal cortex: focus on the cystine glutamate exchanger and group I metabotropic
7
8 glutamate receptors. *J Pharmacol Exp Ther* 314:139–147.
9
10
11 Miele M, Boutelle MG, Fillenz M (1996) The source of physiologically stimulated glutamate
12
13 efflux from the striatum of conscious rats. *J Physiol (Lond)* 497:745-751.
14
15
16 Moghaddam B (2002) Stress activation of glutamate neurotransmission in the prefrontal cortex:
17
18 implications for dopamine-associated psychiatric disorders. *Biol Psychiat* 51: 775-787.
19
20
21 Moran MM, McFarland K, Melendez RI, Kalivas PW, Seamans JK (2005) Cystine/Glutamate
22
23 exchange regulates metabotropic glutamate receptor presynaptic inhibition of excitatory
24
25 transmission and vulnerability to cocaine seeking. *J Neurosci* 25:6389–6393.
26
27
28 Murthy VN, Sejnowski TJ (1997) Heterogeneous release properties of visualized individual
29
30 hippocampal synapses. *Neuron* 18:599–612.
31
32
33 Nicholson C (2001) Diffusion and related transport mechanism in brain tissue. *Rep Prog Physics*
34
35 64:815-884.
36
37
38 Nicholson C, Sykova E (1998) Extracellular space structure revealed by diffusion analysis.
39
40 *Trends Neurosci* 21:207-215.
41
42
43 Patneau DK, Mayer ML (1990) Structure-activity relationships for amino acid transmitter
44
45 candidates acting at N-methyl-D-aspartate and quisqualate receptors. *J Neurosci* 10:2385-
46
47 2399.
48
49
50 Peters YM, O'Donnell P, Carelli RM (2005) Prefrontal cortical cell firing during maintenance,
51
52 extinction, and reinstatement of goal-directed behavior for natural reward. *Synapse* 56(2):74-
53
54 83.
55
56
57
58
59
60
61
62
63
64
65

- 1
2
3
4 Pierce RC, Bell K, Duffy P, Kalivas PW (1996) Repeated cocaine augments excitatory amino
5
6 acid transmission in the nucleus accumbens only in rats having developed behavioral
7
8 sensitization. *J Neurosci* 16(4):1550-1560.
9
10
11 Pow DV (2001) Visualizing the activity of the cystine-glutamate antiporter in glial cells using
12
13 antibodies to aminoadipic acid, a selectively transported substrate. *Glia* 34:27-38.
14
15
16 Reid MS, Berger SP (1996) Evidence for sensitization of cocaine-induced nucleus accumbens
17
18 glutamate release. *Neurosci Lett* 7:1325-1329.
19
20
21 Robinson TE, Kolb B (2004) Structural plasticity associated with exposure to drugs of abuse.
22
23 *Neuropharmacol* 47: 33-46.
24
25
26 Rusakov DA, Kullmann DM (1998) Extrasynaptic glutamate diffusion in the hippocampus:
27
28 ultrastructural constraints, uptake, and receptor activation. *J Neurosci* 18:3158-3170.
29
30
31 Rusakov DA (2001) The role of perisynaptic glial sheaths in glutamate spillover and
32
33 extracellular Ca^{2+} depletion. *Biophys J* 81:1947-1959.
34
35
36 Saftenku EE (2005) Modeling of slow glutamate diffusion and AMPA receptor activation in the
37
38 cerebellar glomerulus. *J Theo Bio* 234: 363-382.
39
40
41 Sato K, Keino-Masu K, Masu M, Bannai S (2002) Distribution of cystine/glutamate exchange
42
43 transporter, system xc-, in the mouse brain. *J Neurosci* 22:8028-8033.
44
45
46 Schoepp DD, True RA (1992) 1S-3R-ACPD-sensitive (metabotropic) [3H] glutamate receptor
47
48 binding in membranes. *Neurosci Lett* 145:100-104.
49
50
51 Sun W, Rebec GV (2006) Repeated cocaine self-administration alters processing of cocaine-
52
53 related information in rat prefrontal cortex. *J Neurosci* 26:8004-8008.
54
55
56
57
58
59
60
61
62
63
64
65

- 1
2
3
4 Swanson CJ, Baker DA, Carson D, Worley PF, Kalivas PW (2001) Repeated cocaine
5 administration attenuates group I metabotropic glutamate receptor-mediated glutamate
6 release and behavioral activation: A potential role for Homer1b/c. *J Neurosci* 21: 9043-9052.
7
8
9
10
11 Sykova E (2004) Extrasynaptic volume transmission and diffusion parameters of the
12 extracellular space. *Neuroscience* 129:861-876.
13
14
15
16 Szumlinski KK, Abernathy KE, Oleson EB, Kullmann M, Lominac KD, He DY, Ron D, During
17 M, Kalivas PW (2006) Homer isoforms differentially regulate cocaine-induced
18 neuroplasticity. *Neuropsychopharmacol* 4:768-77.
19
20
21
22
23 Thorne RG, Nicholson C (2006) In vivo diffusion analysis with quantum dots and dextrans
24 predicts the width of brain extracellular space. *Proc Natl Acad Sci USA* 103: 5567-5572.
25
26
27
28 Timmerman W, Westerink BH (1997) Brain microdialysis of GABA and glutamate: what does it
29 signify. *Synapse* 27:242-261.
30
31
32
33 Trantham H, Szumlinski K, McFarland K, Kalivas PW, Lavin A (2002) Repeated cocaine
34 administration alters the electrophysiological properties of prefrontal cortical neurons.
35
36
37
38
39
40
41 Trommershauser J, Schneggenburger R, Zippelius A, Neher E (2003) Heterogeneous Presynaptic
42 release probabilities: functional relevance for short-term plasticity. *Biophys J* 84:1563-69.
43
44
45
46 Volynski KE, Rusakov DA and Kullmann DM (2006) Presynaptic fluctuations and release-
47 independent depression. *Nat Neurosci* 9:1091-1093.
48
49
50
51 Wadiche JI, Arriza JL, Amara SG, Kavanaugh MP (1995) Kinetics of a human glutamate
52 transporter. *Neuron* 14: 1019-1027.
53
54
55
56 Warr O, Takahashi M, Attwell D (1999) Modulation of extracellular glutamate concentration in
57 rat brain slices by cystine-glutamate exchange. *J Physiol* 514:789-793.
58
59
60
61
62
63
64
65

1
2
3
4 Wyatt I, Gyte A, Simpson MG, Widdowson PS, Lock EA (1996) The role of glutathione in L-2-
5
6 chloropropionic acid induced cerebellar granule cell necrosis in the rat. Arch Tox 70(11):724-
7
8
9 735.

10
11 Xi ZX, Baker DA, Shen H, Carson DS, Kalivas PW (2002) Group II Metabotropic glutamate
12
13 receptors modulate extracellular glutamate in the nucleus accumbens. J Pharmacol Exp Ther
14
15
16 300:162–171.
17
18
19
20
21
22
23
24
25
26
27
28
29
30
31
32
33
34
35
36
37
38
39
40
41
42
43
44
45
46
47
48
49
50
51
52
53
54
55
56
57
58
59
60
61
62
63
64
65

Table 1. Ranges for parameter values used in model.

Parameter	Range of Values (citation)	Model Value ^a
Diffusion coefficient ($\mu\text{m}^2/\text{ms}$)	0.05 – 0.41 (Rusakov and Kullmann, 1998, Saftenku, 2005)	0.05
k_1 ($\text{M}^{-1}\text{ms}^{-1}$)	10^4 (Lehre and Rusakov, 2002)	10^4
k_{-1} (ms^{-1})	0.2 (GLAST/GLT; Lehre and Rusakov, 2002)	0.2
k_2 (ms^{-1})	0.1 (Lehre and Rusakov, 2002)	0.1
No. of molecules per release	4,700 - 80,000 (Bruns and Jahn, 1995)	10,000
Intersynaptic distance (μm)	2-20 (Rusakov, 2001)	2
K_d for mGluR2/3 (μM)	0.1-0.3 (Schoepp and True, 1992)	0.187
Maximum release probability	0.1-0.5 (Trommerhauser et al., 2003; Billups et al., 2005; Volynski et al., 2006)	0.4
XAG conc. (molecules/ μm^2) ^b	550-3780 (Bergles and Jahr, 1997; Lehre and Danbolt, 1998; Colombo, 2005)	see 'b' below
xc^- ($\text{mmol l}^{-1}\text{hr}^{-1}$) ^c	5 – 50 (basal values from Warr et al., 1999; Baker et al., 2003)	41

^a Values used to populate model in figure 1 to generate the data shown in figure 2

^b surface density (molecules/ μm^2) of XAG was distributed as follows: G1a-1575, G1b-970, G2a-790, G2b-560, G3a-260, G3b-150, G4a-0, G4b-0; corresponding volume density ($\times 10^{-21}$ moles) of XAG: G1a-1.089, G1b-1.085, G2a-1.082, G2b-1.08, G3a-0.602, G3b-0.463, G4a-0, G4b-0

^c xc^- was distributed uniformly in seven compartments of G4b: ($i=12, j = 2-8$)

Table 2. Parameters altered by chronic cocaine administration.

Parameter	Control	Cocaine	Reference
Glutamate concentration at P _{ex} (μM; basal)	5.6 ± 1.0	2.89 ± .34	Baker et al., 2003; Szumlinski et al., 2006
Peak glutamate in P _{ex} (μM; during food seeking/cocaine-seeking)	5.6 ± 1.0	13.3 ± 1.4	McFarland et al., 2003, 2004
xc- (mmol l ⁻¹ hr ⁻¹)	41	^a 20.5	Baker et al., 2003; figure 5C
Release probability	0.14 (basal)	^b 0.34 (basal)	Xi et al., 2002
Firing freq (Hz) (basal)	2	1	Sun and Rebec, 2006; Trantham et al., 2002
Firing freq (Hz) (drug-seeking)	N/A	3-15	Chang et al., 1997; Sun and Rebec, 2006

^a Based upon increase in K_m for cystine from 2.1±0.2 to 4.2±0.2 μM; 28.3±7.9% reduction in catalytic subunit of xc- (xCT)

^b Based upon 70% reduction in mGluR2/3 induced GTPγS binding

Table 3. Model predictions at varying firing frequencies using control and chronic cocaine parameters.

Parameter	Control basal	Control biological reward seeking	Cocaine basal^a	Cocaine drug seeking^a
Firing freq (Hz)	2	15	1	15
Release probability	0.14	0.12	0.34	0.30
XAG (moles)	5.4×10^{-21}	5.4×10^{-21}	3.24×10^{-21}	3.24×10^{-21}
xc- ($\text{mmol l}^{-1}\text{hr}^{-1}$)	41	41	20.5	20.5
Estimates of steady state Glu concentrations at three locations				
P_{syn} (μM)	0.16	0.19	0.24	1.05
P_{mGluR} (μM)	0.195	0.28	0.27	1.19
P_{ex} (μM)	5.04	6.58	3.03	12.4

^a Cocaine-induced reduction in XAG (40%), xc- (50%) and mGluR2/3 signaling (70%; modeled as release probability)

Figure Legends

Figure 1. The glial configuration used to study glutamate homeostasis in the perisynaptic space around the PFC-accumbens synapse. The model depicts glutamate transporters (XAG) and cystine-glutamate exchangers (xc-) in glial regions (shaded) in varying concentrations. The cleft ($\delta=20$ nm) separates the two hemispheres of radius ($r = 160$ nm) surrounded by glial sheaths (G_i , $i=1-4$; $i=1$ being the closest to the synapse) with the highest density of XAG in G_1 and decreasing in radially outward sheaths. Each sheath is 50 nm thick with an impermeable surface in the middle, and with XAG volume-populated in the 25 nm thick space on either side, permitting interaction with glutamate molecules in those regions. The perisynaptic space is partitioned in radial (step $\sigma =25$ nm) and tangential (step $\theta =20^\circ$) directions as in Rusakov (2001). Binding, uptake and efflux are computed for each compartment. Glutamate concentrations were measured at three sites, within the synaptic cleft (at P_{syn}), in the perisynaptic region containing presynaptic mGluR2/3 (at P_{mGluR}), and at the site where dialysis probe measures extracellular glutamate (at P_{ex}).

Figure 2. Concentrations of glutamate at different spatial locations under control conditions. **A.** The increase in glutamate at P_{ex} remained within the basal range over the entire 1-15 Hz range of firing. **B.** As firing frequency increases, the concentration of glutamate in the vicinity of perisynaptic mGluR2/3 autoreceptors (at P_{mGluR}) increases producing a concomitant decrease in release probability. **C.** Model output at 2 and 15 Hz over 5 sec, illustrating the dynamic changes in synaptic (at P_{syn}), and extracellular glutamate (at P_{ex}).

1
2
3
4 **Figure 3.** Effect of reducing XAG on the concentration of extracellular glutamate at P_{ex} , in
5 cocaine treated rats. To model the cocaine condition, the function of xc- and mGluR2/3 were
6 reduced by 50% and 70%, respectively. Iterations of the model were then run at different
7 percent decreases in the concentration of XAG over a firing frequency range of 1-15 Hz.
8
9
10
11
12
13
14

15
16 **Figure 4.** Concentrations of glutamate at three spatial locations under cocaine conditions (i.e.,
17 xc- reduced 50%, mGluR2/3 signaling reduced 70%, XAG reduced 40%). **A.** The increase in
18 glutamate at P_{ex} was within the basal range at 1 Hz and increases to the cocaine-seeking range at
19 15 Hz firing frequency. **B.** As firing frequency increased, the concentration of glutamate in the
20 vicinity of perisynaptic mGluR2/3 autoreceptors (at P_{mGluR}) increased with a concomitant
21 decrease in release probability. **C.** Model output at 1 and 15 Hz over 5 sec, illustrating the
22 dynamic changes in synaptic (at P_{syn}), and extracellular concentration (at P_{ex}).
23
24
25
26
27
28
29
30
31
32
33
34
35
36
37
38
39
40
41
42
43
44
45
46
47
48
49
50
51
52
53
54
55
56
57
58
59
60
61
62
63
64
65

Figure 1
[Click here to download high resolution image](#)

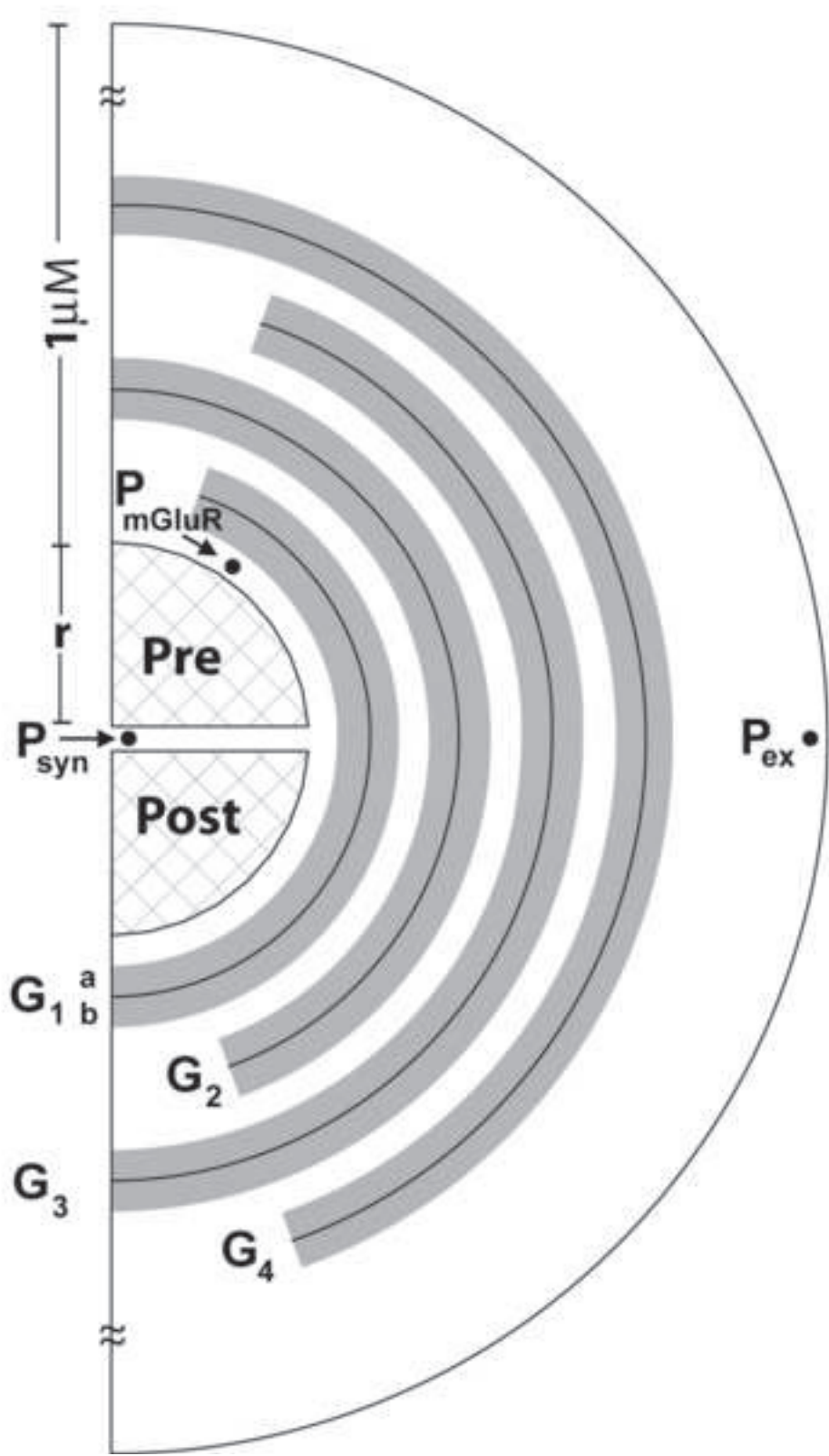


Figure 2
 Click here to download high resolution image

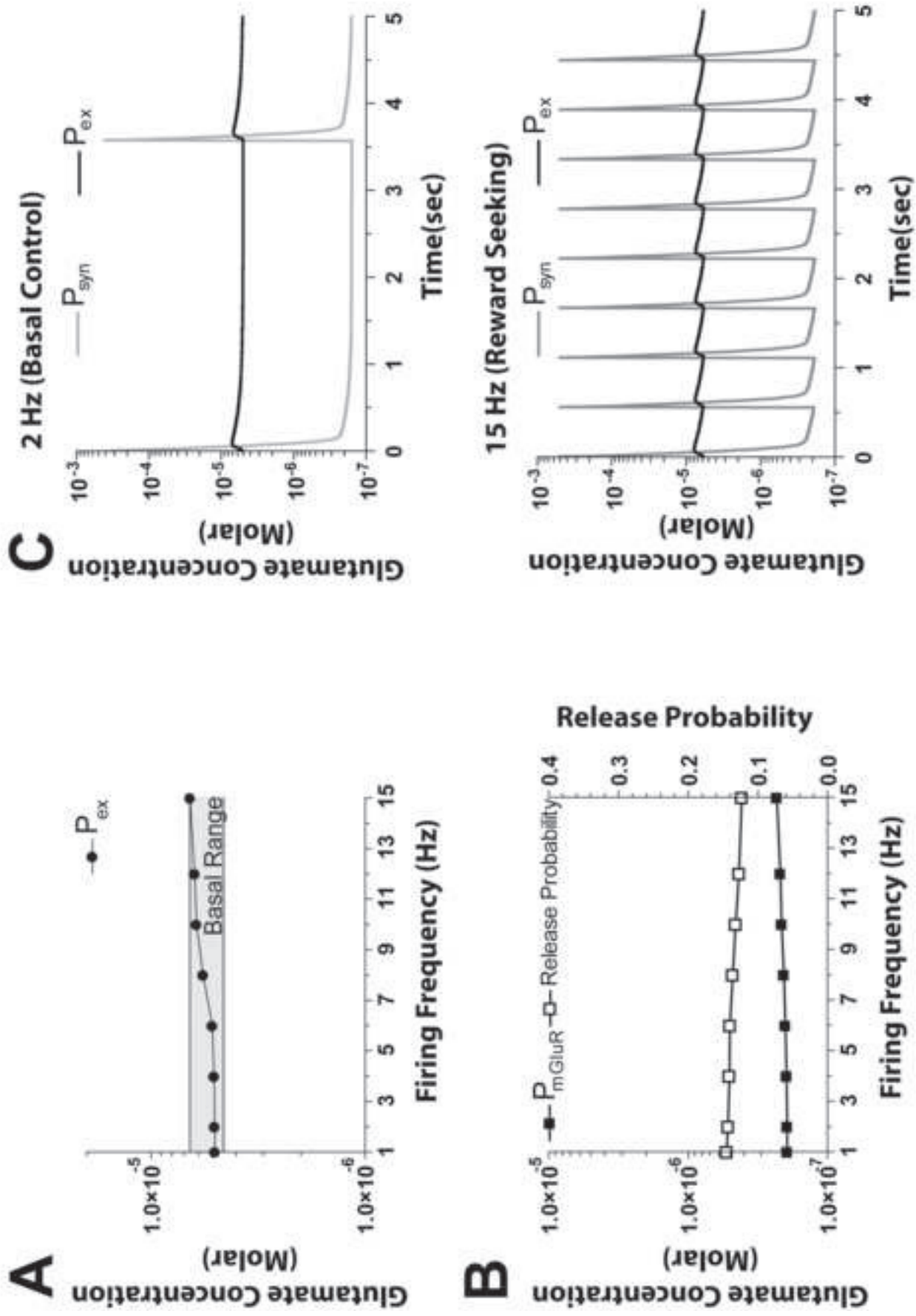


Figure 3

[Click here to download high resolution image](#)

